scientific reports

Check for updates

OPEN

Periostin mediates collagen production, ECM remodeling and myofibroblast differentiation in breast prosthesis capsule formation

Ying Yang[1,4]✉, Shumo Li[2,4], Li Bian[1], Xiaoming Dai[3], Jun Hu[1], Yun Ma[2] & Zhiyuan Wang[1]

Capsular contraction is the most common complication after breast augmentation or reconstruction, and is the main reason underlying patient dissatisfaction and additional subsequent surgeries. Periostin is an extracellular matrix protein and a member of TGF-β superfamily. Studies have shown that periostin is closely related to fibrosis, collagen cross-linking and tissue remodeling. In this study, we observed the expression of periostin and other fibrosis-related proteins in the capsule of human breast silicon implant, assessing their relationship with the extent of capsule fibrosis. By using human breast derived fibroblasts with manipulated periostin expression level, we explored periostin's impact on other fibrosis-related cytokines, fibroblast proliferation, differentiation, and collagen synthesis. Furthermore, we employed a murine model of prosthesis implantation to elucidate the roles of periostin and lysyl oxidase (LOX) in capsule formation. Immunohistochemical analysis of clinical capsular specimens revealed a significant correlation between periostin expression levels and the severity of capsular contracture. In vitro experiments using human breast-derived fibroblasts demonstrated that periostin promotes fibroblast proliferation and regulates the expression of key fibrosis-related proteins such as LOX, BMP-1, fibronectin, and tenascin-C at both protein and mRNA levels. Moreover, periostin was found to induce fibroblast differentiation into myofibroblasts and enhance collagen production. In the murine model of prosthesis implantation, periostin and LOX were observed to increase the thickness of the prosthesis capsule, whereas the administration of the LOX inhibitor β-aminopropionitrile (BAPN) significantly attenuated capsule formation. Our study underscores the significant role of periostin in the pathogenesis of breast prosthesis capsule formation and contracture. These findings provide novel insights into the mechanisms underlying capsular contracture and suggest periostin as a potential therapeutic target for mitigating this complication.

Keywords Breast implants/Adverse effects, Silicon implant, Capsular contraction, Periostin, Fibroblasts, Animals

Abbreviations

ROC	Receiver operating characteristic curve
α-SMA	Alpha smooth muscle actin
BMP	Bone morphogenetic protein
ECM	Extracellular matrix
GAPDH	Glyceraldehyde-3-phosphate dehydrogenase
HE	Hematoxylin and eosin
HRP	Horseradish peroxidase
KM	Kunming
LOX	Lysyl oxidase
LOXL	Lysyl oxidase-like
MOI	Multiplicity of infection
PBS	Phosphate-buffered saline

[1]Department of Pathology, The First Affiliated Hospital of Kunming Medical University, Kunming, China. [2]Department of Breast Surgery, The First Affiliated Hospital of Kunming Medical University, Kunming, China. [3]Department of Plastic Surgery, The First Affiliated Hospital of Kunming Medical University, Kunming, China. [4]co-first authors: Ying Yang and Shumo Li. ✉email: yangyingou@163.com

PVDF	Polyvinylidene fluoride
qRT-PCR	Quantitative real-time polymerase chain reaction
RIPA	Radioimmunoprecipitation assay
SD	Standard deviation
SDS-PAGE	Sodium dodecyl sulfate-polyacrylamide gel electrophoresis
shRNA	Short hairpin RNA
TGF-β	Transforming growth factor-beta

After decades of continuous upgrading, silicone prostheses have become the most commonly used type of implant in breast augmentation surgery. Capsular contraction represents the most prevalent complication after breast augmentation, serving as the major reason underlying patient dissatisfaction and additional subsequent surgeries. Reported incidence of capsular contraction have varied, ranging from 2.8 to 20.4% in previous reports[1,2]with isolated reports indicating rates as high as 80%[3]. Capsule is the fibrous tissue around the surgical implants or prostheses. The formation of the capsule is like the two sides of a coin: it holds the implant in place and causes the pain, sclerosis, lumps and malformation at the same time. Presently, effective preventative and therapeutic strategies remain elusive, necessitating reoperation in cases of severe capsular contracture, thereby inflicting significant physical and psychological trauma upon patients[4].

The formation of fibrous envelope is the body's protective response to exogenous implants and typically occurs within 1 to 2 weeks after operations. The main component cells of the capsule include fibroblasts, myofibroblasts and inflammatory cells such as macrophage, polymorpnonuclear leukocytes, lymphocytes, plasma cells and mastocytes[5]. Numerous factors influence the development of capsular contracture, encompassing surgical techniques, implant characteristics, infectious agents, and other variables contributing to contracture pathogenesis[6]. Despite extensive research, the precise mechanisms governing capsule formation and contracture remain incompletely understood. Overall, exogenous implants incite inflammation, prompting fibroblast-mediated collagen deposition, and myofibroblast-induced tissue contraction. When the physiological wound healing process stagnates, pathological changes ensue, culminating in capsular contracture[7]. A large number of studies, including implant types, surface characteristics, surgical methodologies, and bacterial infections, have endeavored to elucidate the intricate mechanisms of capsule formation and contracture, in order to seek effective therapeutic and preventative methods[8–10].

Periostin, a 90 kDa secreted glycoprotein encoded by the *Postn* gene, is a member of the transforming growth factor-beta (TGF-β) protein-induced superfamily with very low expression in normal adult tissues but strongly mediated secretion into the extracellular interstitium after acute injury[11]. Extensive literature has studied the important role of periostin in a variety of areas, including bone regeneration, bone marrow fibrosis, myocardial infarction recovery, airway inflammation, idiopathic pulmonary fibrosis, muscle atrophy and fibrosis, kidney disease, skin inflammation, joint stiffness, and tumor progression, invasion, metastasis, and fibrosis[12–14]. Previous studies have highlighted periostin's ability to augment active lysyl oxidase (LOX) levels, thereby facilitating collagen cross-linking and enhancing connective tissue mechanical properties[15]. Given its central involvement in fibrotic processes, we hypothesize that periostin may play a crucial regulatory role in capsule formation and contractures, although no prior reports have explored its specific contribution to these processes following breast prosthesis implantation. Consequently, our study observed the expression of periostin and its correlation with the degree of capsule contracture within the capsule of human breast silicone implants. By using human breast derived fibroblasts with manipulated periostin expression, we investigated its impact on other fibrosis-related cytokines, fibroblast proliferation, differentiation, and collagen synthesis. Additionally, we employed a murine model of prosthesis implantation to validate the roles of periostin and LOX in capsule formation.

Materials and methods

Study design

In the clinical part, capsule specimens from breast implants were collected, clinicopathological characteristics and the extent of capsular contraction were analyzed, and the immunnohistochemistry were performed to compare the expression of periostin and other fibrosis-related proteins between different contracture degree groups. In the in vitro experiment part, using human breast derived fibroblasts with up and down regulation of periostin expression, we investigated its impact on other fibrosis-related cytokines, fibroblast proliferation, differentiation, and collagen synthesis. In the animal experiment section, 60 mice were randomly divided into 4 groups and received treatment with silicone prosthesis implantation plus periostin, LOX, BAPN, and physiological saline control, respectively to compare the effects of these treatments on the prosthesis capsule.

Clinical cases collection and grouping

We collected all specimens submitted for breast silicone prosthesis removal surgery and prosthesis capsule resection surgery spanning from 2009 to 2019, excluding specimens not of breast origin and those related to other types of prostheses. The sample size was determined by reference[16]. Clinical and radiological data associated with these cases were systematically compiled. All of the cases were grouped according to the degree of capsule contracture employing Baker grading system[5](Grade I denoting normal breast appearance and touch; Grade II indicating mild contracture perceptible to the surgeon but lacking symptoms; Grade III indicative of moderate contracture, characterized by palpable firmness; and Grade IV representing severe contracture, visually apparent with symptomatic manifestations).

Clinicopathological eveluation

Formalin-fixed, paraffin-embedded tissue sections stained with hematoxylin and eosin (HE) were examined under a microscope. Microscopic assessments encompassed various features, including thickness of collagen

layer, inflammation type and severity, fiber orgnization, calcification and morphological characteristics of breast glands within the specimens. Since previous studies have shown that the Baker grade is unreliable as a diagnostic tool due to low interobserver reliability[17]we used the histopathological scoring system proposed by Larsen et al. for patients with breast augmentation to perform semi quantitative scoring of histological features[18,19]which gave a combined maximum score of 26 points for every specimen.

Antibodies

Rabbit polyclonal anti-periostin antibodies (Abcam, ab14041), mouse monoclonal anti-alpha smooth muscle actin (α-SMA) antibodies (Abcam, ab7817), rabbit polyclonal anti-Fibronectin antibodies (Proteintech, 15613-AP), rabbit polyclonal anti-LOX antibodies (Proteintech, 17958-1-AP), rabbit polyclonal anti-bone morphogenetic protein 1 (BMP1) antibodies (Affinity, DF9280), rabbit recombinant anti-beta-Actin antibodies (Proteintech, 81115-1-RR) and rabbit monoclonal anti-Tenascin-C antibodies (CST, 12221) were purchased from the sources indicated.

Immunohistochemistry

Capsule tissues surrounding breast implants were sectioned, dewaxed, subjected to antigen retrieval, and then cooled. Endogenous peroxidases were neutralized using 3% hydrogen peroxide (H_2O_2). Subsequently, sections were incubated with primary antibodies for 1 h at room temperature, followed by incubation with secondary antibodies for 40 min at room temperature. Visualization was achieved through DAB staining, complemented by hematoxylin nuclear staining. Following dehydration, clearing, and mounting, image analysis was conducted utilizing Image-proplus software (Media Cybernetics, USA), with the intensity of staining quantified as the product of positive grey value and positive area (IOD). The negative control images are shown in Supplementary Fig. 1. Ovarian tissue were used as a negative control for periostin and α-SMA, normal breast glandular epithelial cells were used as a negative control for LOX, fibronectin and tenascin-C, and ruptured implant was used as a negative control for BMP-1 because the expression of BMP-1 is ubiquitous.

Cell culture

Human breast-derived fibroblasts (HMF7630) obtained from CELLBIO, Shanghai, and the 293T cell line sourced from the Kunming Institute of Zoology were utilized in this study. The cells were cultured in RPMI-1640 medium (Gibco, Thermo Fisher Scientific) supplemented with 10% fetal bovine serum (Gibco) at 37 °C in a humidified atmosphere with 5% CO2. Medium was refreshed every 24 h, and cells were harvested during the logarithmic growth phase for subsequent experiments.

Plasmid and cell transfection

Periostin expression and interference vectors were synthesized by GeneCopoeia (Guangzhou, China, see Fig. 3). The sequences of short hairpin RNA (shRNA) are detailed in Table 1. Following identification and screening, periostin expression, interference, and negative control plasmids were packaged with lentivirus in human embryonic kidney 293T cells using the Lenti-Pac™ HIV Expression Packaging Kit (GeneCopoeia, Guangzhou, China). HMF7630 cells were transfected with recombinant lentivirus at a multiplicity of infection (MOI) of 5, at a growth density of 75%. Stably transfected cells were selected in the presence of 2 μg/ml puromycin until the infection positivity rate exceeded 80%.

RNA isolation and quantitative real-time polymerase chain reaction (qRT-PCR)

Total RNA was extracted from cells using Trizol reagent (MRC, Germany) as per the manufacturer's protocol, followed by reverse transcription to synthesize first-strand cDNA using the All-in-OneTM First-Strand-cDNA Synthesis Kit (GeneCopoeia, USA). Specific primer sets for periostin, LOX, BMP-1, Fibronectin, Tenascin C, and glyceraldehyde-3-phosphate dehydrogenase (GAPDH) were designed (Table 2). Quantitative real-time polymerase chain reaction (qRT-PCR) was conducted using the All-in-One™ qPCR Mix (GeneCopoeia, USA) on a Real-Time PCR Detection System (2720 Thermo, USA). All experiments were independently replicated three times, with relative mRNA levels normalized to endogenous GAPDH mRNA using the relative quantification comparative Ct method.

Western blot analysis

Transfected cells were washed with phosphate-buffered saline (PBS) and lysed in radioimmunoprecipitation assay (RIPA) buffer containing protease inhibitor. The resulting supernatant was collected and stored at -80 °C. Protein samples were subjected to sodium dodecyl sulfate-polyacrylamide gel electrophoresis (SDS-PAGE), transferred to polyvinylidene fluoride (PVDF) membranes, and blocked with 5% skim milk for 1 h. Membranes were then incubated with specific primary antibodies at room temperature for 2 h. Following incubation with

Name	Sense (5′-3′)
shPeriostin-a	GCTGCTTATTGTTAACCCTAT
shPeriostin-b	GCACTTGTAAGAACTGGTATA
shPeriostin-c	GCAACGTGAATGTTGAATTAC
shPeriostin-d	GGTGACAGTATAACAGTAAAT

Table 1. Sequences of shRNA.

Gene (Homo)	Sequence (5′–3′)	
POSTN	Forward	CCAAATGTCTGTGCCCTTC
	Reverse	CCCTTTCCCTCGATCTCCT
LOX	Forward	TAGCCACTATGACCTGCTTGAT
	Reverse	CTGGGGTTTACACTGACCTTTA
BMP-1	Forward	TGCGGGGGTGATGTGAAAA
	Reverse	CTGGGTAGTTGGGCGATTG
Fibronectin	Forward	TTCCCATTATGCCGTTGGAG
	Reverse	GAAATGACCACTTCCAAAGCCTA
Tenascin-C	Forward	ACATCGCATCAACATCCCC
	Reverse	TCCTCCAGTCTGCTCAGCA
GAPDH	Forward	CGCTGAGTACGTCGTGGAGTC
	Reverse	GCTGATGATCTTGAGGCTGTTGTC

Table 2. Sequences of primers used for qRT-PCR.

secondary horseradish peroxidase (HRP)-conjugated antibodies (dilution 1:4000) for 1.5 h at room temperature, membranes were washed thrice with Tris-buffered saline with Tween (TBST), incubated with Immobilon Western Chemiluminescent horseradish peroxidase substrate (Millipore), and exposed to medical x-ray film (Carestream).

CCK8 assay

Cells in logarithmic growth phase were detached with trypsin and centrifuged. The cell number was determined in a cell counting plate, and the digested cells were adjusted to 5×10^4 cells/ml. Subsequently, cells were inoculated into a 96-well cell culture plate at a rate of 5×10^3 cells/well (100 µl per well), with three wells allocated for each cell group simultaneously. At 0 h, 24 h, 48 h, and 72 h post-inoculation, 10 µl of CCK-8 solution was added to each well. After 2 h of incubation at 37 °C and 5% CO_2, absorbance at 450 nm was measured.

Immunofluorescence microscopy

Cells from selected cell lines in logarithmic growth phase were detached with trypsin and centrifuged to prepare a 10^5 cell suspension. Subsequently, 1 ml of each suspension was plated onto a 24-well cell slide (three wells per cell line). After cell adherence, slides were removed from the incubator, washed three times with PBS, and fixed in 4% paraformaldehyde in PBS for 30 min at room temperature. Following PBS washes, cells were blocked with 5% bovine serum albumin for 30 min at 37 °C. Primary antibody (α-SMA:1/100) was then applied and incubated overnight at 4 °C in 2% bovine serum albumin. After washing, cells were incubated with fluorescence-tagged secondary antibodies (Goat Anti-Mouse IgG H&L Alexa Fluor® 647; 1:2000) for 1 h at 37 °C, followed by additional PBS washes. Nuclei were stained with DIPA (Molecular Probes, Invitrogen), and fluorescent images were captured using a fluorescence microscope (BX61; Olympus, Japan).

Hydroxyproline measurement

To assess periostin's impact on collagen content, hydroxyproline levels were measured in cell lines. Five million stable screened cell lines were taken seperately and 1 ml of extraction solution was added. Complete hydrolysis was achieved by boiling or digesting samples at 110 °C oven for 2–6 h until it became visually transparent. Following hydrolysis, samples were centrifuged (16,000 rpm, 25 °C, 20 min) to pellet insoluble debris. The resulting supernatant was then neutralized to pH 6–8 using approximately 0.5 ml of 10 mol/L NaOH and diluted to a final volume of 2 ml with distilled water prior to analysis. For spectrophotometric measurement, the instrument was preheated for a minimum of 30 min and calibrated to a wavelength of 560 nm. A standard curve was prepared by serially diluting the hydroxyproline standard solution to concentrations of 30, 15, 7.5, 3.75, 1.875, 0.938, 0.469, and 0.234 µg/mL. Absorbance readings of both standards and neutralized sample supernatants were recorded at 560 nm against a distilled water blank. Hydroxyproline content within the cell lines was subsequently calculated based on the generated standard curve.

Animal experiments

The mice were purchased from SiPeiFu (Beijing) Biotechnology Co., LTD. License number: SCXK(Beijing)2019-0010. Sixty female Kunming (KM) mice aged 6–8 weeks were divided into four groups using random number table: silicone + physiological saline, silicone + periostin, silicone + LOX, and silicone + BAPN, with 15 mice per group. Each group underwent the following procedure: after anesthesia induction(isoflurane inhalant anesthesia), incisions were made bilaterally 0.5 cm from the midline of the back to expose the skin and sarcolemma, creating 1.5 cm pockets. Disinfected 1 ml hemispherical silicone implants were inserted, and incisions were closed. Mice received subcutaneous injections of periostin, LOX, LOX inhibitor BAPN, or control physiological saline around the prosthesis, administered once daily at a dose of 200 mg/kg for 30 days. Weekly photographs were taken to monitor wound surface changes. After 30 days, silicone prostheses and surrounding tissues of all the mice were excised for further analysis without exclusion. Capsule thickness was measured and WB and QPCR were performed to analyse the expression of periostin and other fibrosis-related genes. To avoid the influence of confounding factors, all animals were raised in the same way and in the same place, using the

same treatment method except for intervention drugs. The experimental operator was unaware of the group allocation throughout the entire experiment period. The sample size was determined by reference[20].

Statistical analysis and software

Statistical analysis were performed using Statistical Product and Service Solutions (SPSS, version 26.0, IBM, New York, USA). Continuous variables were expressed as the mean ± standard deviation (SD) and were analyzed by unpaired Student's *t* tests for the comparison of two groups when the variances are equal. Categorical variables were analyzed using the χ^2 test or Fisher's exact test. Level of significance was set at $p < 0.05$. GraphPad Prism (vison 6.0, GraphPad, USA) was used to draw stastistical graphs. ImageJ was employed for grayscale analysis of WB protein bands.

Ethics approval

The study protocol involving human tissues was approved by the Ethics Committee of The First Affiliated Hospital of Kunming Medical University (2024L144). The informed consent was obtained from all participants. All experiments were performed in accordance with the ethical guidelines of the 2013 Declaration of Helsinki. The material was anonymized at the time of collection. Animal care and experiments were conducted in compliance with ARRIVE guidelines and the American Veterinary Medical Association Guidelines for the Euthanasia of Animals (2020), with approval obtained from the Animal Ethics Committee of Kunming Medical University (Kmmu20230546).

Results

Periostin expression in human breast capsules of silicon implants

To assess the association between periostin expression and the extent of capsule contracture, we collected clinical specimens from breast implant cases and analyzed the relationship between periostin expression and clinicopathological characteristics. Twenty-one specimens from 11 patients with breast implants were obtained, comprising 11 classified as Baker Grades I-II and 10 as Baker Grades III-IV based on the clinical degree of capsule contraction. All patients involved Chinese females with a mean age of 42.3 years (range: 29–42). The duration of prosthesis implantation ranged from 1 to 30 years, with an average of 12.6 years. Silicone implants were used in all 11 patients, with 10 patients yielding bilateral breast capsule specimens and 1 patient yielding a unilateral specimen. Clinically, pain or discomfort was reported in 3 patients, breast lumps (including multiple lumps) in 4 patients, breast texture hardening in 2 patients, breast deformation in 4 patients, signs of infection such as swelling and fever in 1 patient, and breast softening with lump formation following a car accident in 1 patient.

Capsule formation was observed in 20 specimens under microscopic examination. The relationship between histological scores and the extent of capsular contraction is summarized in Table 3. The specimens were stratified into 3 groups of progressing severity of the histological implant response according to the histological score: mild implant response (0–9 points), moderate implant response (10–15 points), and severe implant response (16–26 points). Two specimens from a prosthetic rupture caused by a car accident were clinically evaluated as Baker grade IV, but the histological scores were only 3 points, which were considered a false positive in clinical evaluation. After excluding these two cases, the grouping of histological implant responses was significantly correlated with caplular contracture (Baker I/II or III/IV) ($P = 0.047$). Spearman correlation coefficient analysis showed a moderate to strong positive correlation between histological scores and the extent of capsular contraction (Spearman correlation = 0.63, $P = 0.004$) (Fig. 1A). The receiver operating characteristic curve

	Score	Baker I/II (%)	Baker III/IV (%)
No. of breasts		11	10
Thickness of collagen layer (μm)			
< 400	0	0	2 (20%)
400–600	3	4 (36.36%)	1 (10%)
600–800	7	1 (9.09%)	1 (10%)
> 800	10	6 (54.55%)	6 (60%)
Fiber organization			
Highly disorgnized	0	0	2 (20%)
Moderately disorgnized	2	2 (18.18%)	0
Highly orgnized	4	9 (81.82%)	8 (80%)
Inflammatory infiltration			
Few individual inflammatory cells	0	9 (81.82%)	4 (40%)
Several individual inflammatory cells and few aggregates	3	2 (18.18%)	5 (50%)
Several infiltration with several follicular aggregates	6	0	1 (10%)
Calcification			
Absent	0	11 (100%)	7 (70%)
Present	6	0	3 (30%)

Table 3. The relationship between histological scores and clinical capsular contraction.

(ROC) shows that the histological scoring system has strong predictive ability for clinical capsular contracture (AUC = 0.807, Fig. 1B). To elucidate the relationship between capsule contraction extent and periostin expression alongside other fibrosis-related proteins, immunohistochemistry was performed on silicone implant capsules. Immunohistochemistry and image analysis revealed an escalation in the expression of periostin, LOX, fibronectin, Tenascin-C, and α-SMA with worsening capsule contraction (Fig. 2).

Role of Periostin on fibrotic function of human breast derived fibroblasts in vitro

To investigate the impact of periostin on fibroblasts during fibrosis, we constructed both overexpression and interference plasmids. The expression and interference vector maps are depicted in Fig. 3. Validation of the plasmids was conducted using 1% agarose gel electrophoresis, Western blot, and quantitative polymerase chain reaction (qPCR). After 4 weeks of screening, periostin protein and mRNA levels in stably transfected HMF7630 cells were consistent with expectations (Fig. 3).

To assess the regulatory effect of periostin on fibrosis-related genes, we evaluated the expression of LOX, BMP-1, fibronectin, and Tenascin-C in periostin overexpression and interference cell lines. Compared to Ctrl-mPeriostin-HMF7630, both protein and mRNA levels of periostin, LOX, BMP-1, fibronectin, and Tenascin-C significantly increased in the mPeriostin-HMF7630 cell line while markedly decreased in the shPeriostin-HMF7630 cell line (Fig. 4A, B). This confirmed the positive regulatory effect of periostin on LOX, BMP-1, fibronectin, and Tenascin-C.

To explore the association between periostin expression and fibroblast proliferation, we conducted a CCK8 assay. The results indicated that the mPeriostin-HMF7630 cell line exhibited significantly enhanced proliferation compared to the Ctrl-mPeriostin-HMF7630 cell line, while the shPeriostin-HMF7630 cell line showed markedly reduced proliferation compared to the control. These findings suggest that the periostin gene promotes fibroblast proliferation (Fig. 4C).

Immunofluorescence analysis of α-SMA expression in the cell lines revealed significantly higher levels in the mPeriostin-HMF7630 cell line compared to the control (56.26 ± 3.88 vs. 23.01 ± 4.75, $p = 0.0009$), whereas expression was notably lower in the shPeriostin-HMF7630 cell line compared to the control (13.66 ± 1.38 vs. 22.07 ± 2.19, $p = 0.0115$) (Fig. 4D). Given that α-SMA expression serves as a marker for fibroblast differentiation into myofibroblasts, these results suggest that periostin promotes fibroblast differentiation into myofibroblasts.

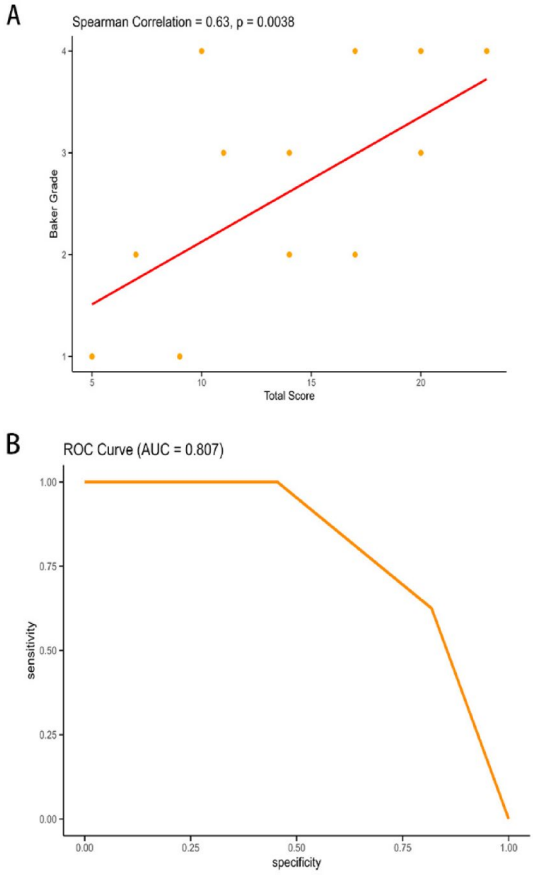

Fig. 1. The relationship between histological scores and capsular contracture ($N = 19$). (**A**) Spearman correlation coefficient analysis showed a moderate to strong positive correlation between histological scores and the extent of capsular contraction. (**B**) The receiver operating characteristic curve (ROC) shows that the histological scoring system has strong predictive ability for clinical capsular contracture.

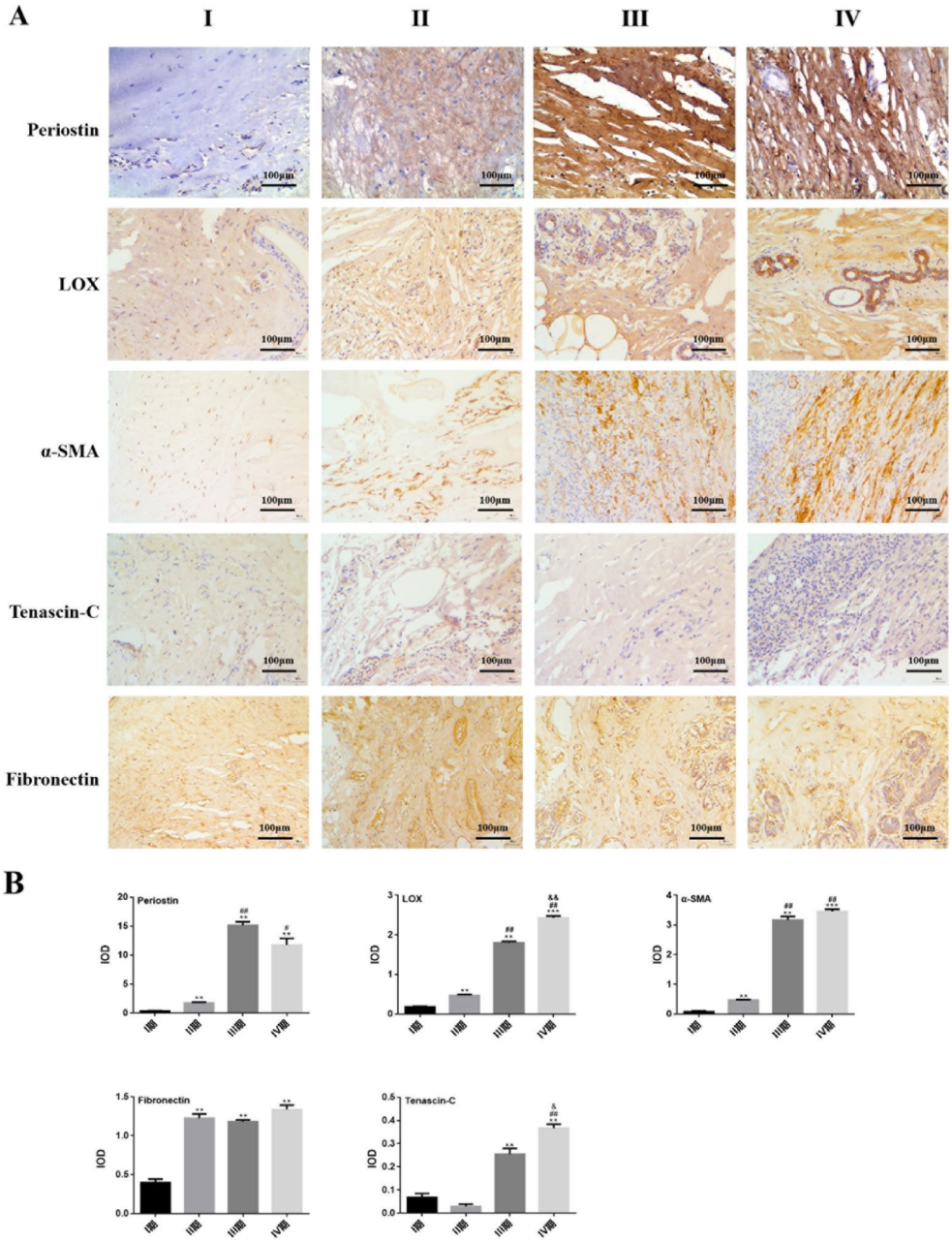

Fig. 2. The immunohistochemical cxpression of periostin and other fibrosis related protein in prosthesis capsules with different degrees of capsular contraction ($N = 19$). (**A**) The immunohistochemical images of periostin, LOX, α-SMA, Tenascin-C and Fibronectin in capsules of Baker grade I to IV. (**B**) The IOD value of immunohistochemical stain of periostin and other fibrosis related markers in capsules of Baker grade I to IV. (Compared with stage I, $^{*}P < 0.05$, $^{**}P < 0.01$, $^{***}P < 0.01$; Compared with stage II, $^{\#}P < 0.05$, $^{\#\#}P < 0.01$; Compared with stage III, $^{\&}P < 0.05$, $^{\&\&}P < 0.01$)

To assess the impact of periostin on collagen content, we measured hydroxyproline levels in the cell lines. The mPeriostin cell strain exhibited significantly higher collagen content compared to the ctrl-mPeriostin cell strain (13.46 ± 2.57 vs. 7.39 ± 0.334, $p = 0.049$). Although not statistically significant, the collagen content in the shPeriostin cell strain appeared lower than the control (5.63 ± 1.34 vs. 7.08 ± 0.18, $p = 0.174$) (Fig. 4E).

Impact of periostin, LOX and inhibitor treatment on capsule formation in mice following prosthetic implantation

To assess the influence of periostin on capsule formation in vivo, we established a mouse prosthesis implantation model and investigated the effects of periostin, LOX, and inhibitor treatment on capsule formation following prosthetic implantation (Fig. 5A). β-aminopropionitrile (BAPN), the most potent inhibitor of LOXs, was utilized as the inhibitor. As illustrated in Fig. 5B, compared to the silica gel + saline group, the silica gel + LOX group

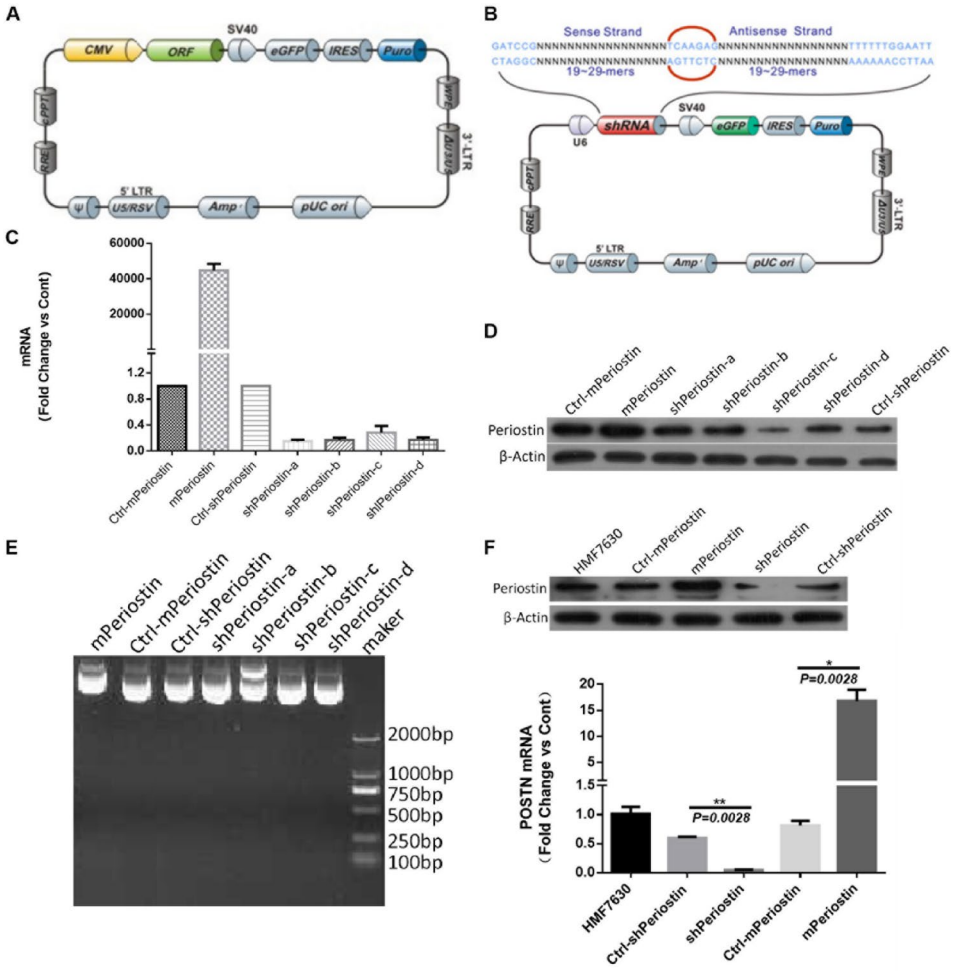

Fig. 3. Identification, screening, lentiviral packaging, and transfection of overexpressing and interfering periostin plasmid vectors. (**A**) Periostin expression vector map. (**B**) Periostin interference vector map. (**C**) The expression of periostin mRNA tested by QPCR 72 h after transfection. (**D**) The expression of periostin protein tested by Western Blot 72 h after transfection. (**E**) The result of the 1% agarose gel electropporesis. (**F**) The expression of periostin protein and mRNA tested by Western Blot and QPCR after lentiviral infection and puromycin screening.

exhibited the slowest wound healing and more severe suppurative conditions. Wound healing was also delayed in the silica gel + Periostin group and silica gel + BAPN group, with mild suppurative conditions observed. Gross examination of the prosthesis block revealed that the silica gel + periostin group had a larger prosthesis block with surrounding tissues appearing yellow compared to the silica gel + saline group. Conversely, the prosthesis blocks of the silica gel + LOX group and silica gel + BAPN group resembled those of the control group, with surrounding tissues displaying slight yellowing (Fig. 5C).

Following 30 days of feeding, capsule tissue was harvested for subsequent experiments. QPCR and Western blot results demonstrated significantly higher expression levels of periostin and other fibrosis-related genes/proteins (LOX, BMP-1, fibronectin, Tenascin-C, and α-SMA) in the silica gel + LOX group and silica gel + periostin group compared to the silica gel + saline group. Conversely, expression levels of these genes/proteins in the silica gel + BAPN group were significantly lower than those in the control group (Fig. 6A, B).

Subsequent to H&E staining of the capsule tissue, capsule thickness was assessed. The mean thicknesses of the silica gel + Periostin group and silica gel + LOX group were significantly greater than that of the silica gel + saline group. Conversely, capsules in the silica gel + BAPN group were notably thinner than those in the control group (Fig. 7A, B). Monocytes, neutrophils, and eosinophils also showed significant increases in the silica gel + LOX and silica gel + Periostin groups (Fig. 7C). Immunohistochemistry of periostin and other fibrosis-related proteins aligned with the results of QPCR and Western blot, indicating an increase in the silica gel + Periostin group and silica gel + LOX group, and a decrease in the silica gel + BAPN group (Fig. 7D).

Discussion

Despite numerous investigations into capsular contracture, the underlying mechanism remains incompletely elucidated. Our study revealed a correlation between periostin expression in clinical capsular specimens and the

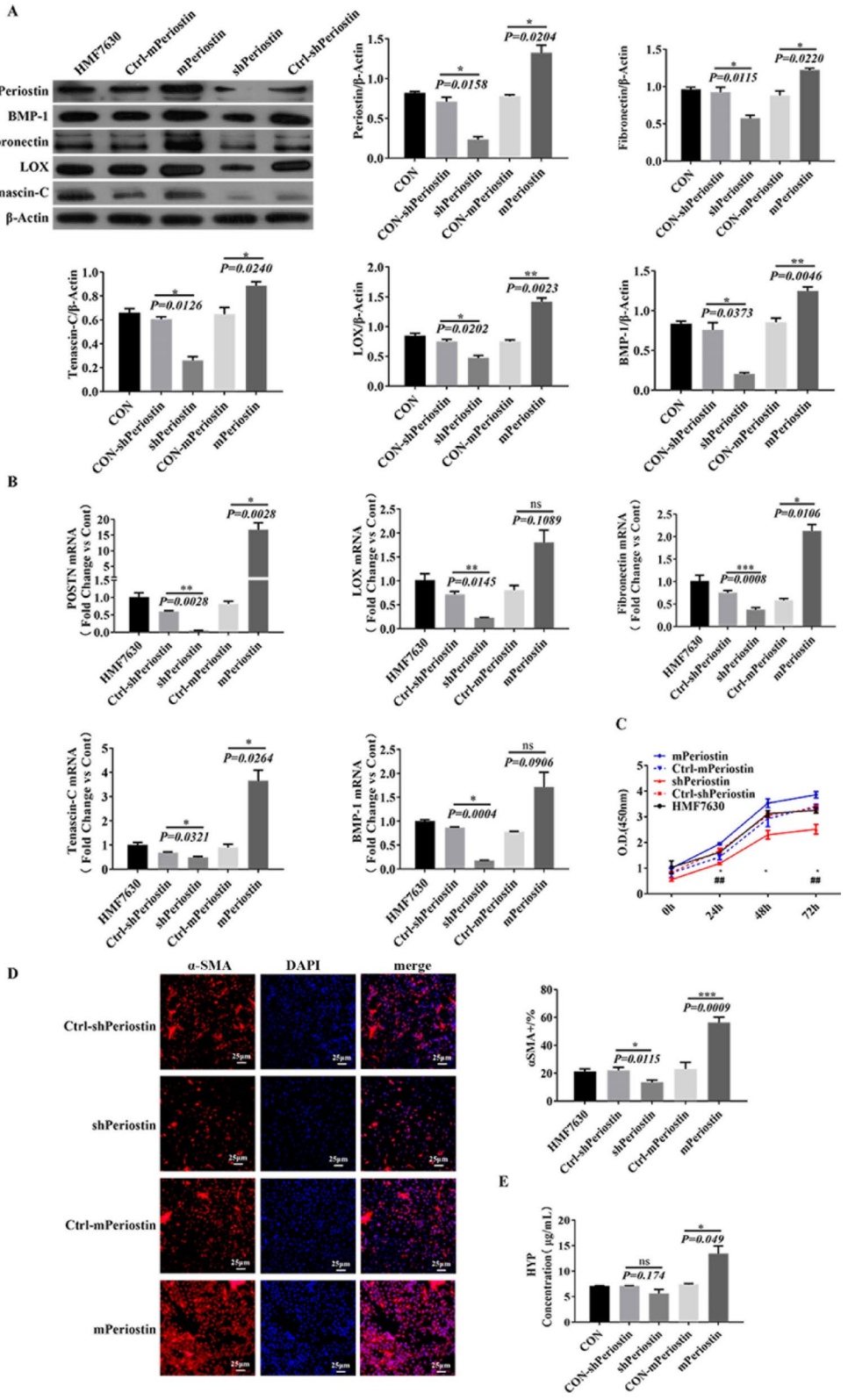

Fig. 4. The expression of periostin and other fibrosis related genes in the cell lines after lentiviral infection and 4-weeks puromycin screening, the proliferation, and the influence on fibrosis related functions. (**A**) Periostin, LOX, BMP-1, Fibronectin and Tenascin-C protein expression were detected by Western Blot. **P*<0.05, ** *P*<0.01; (**B**) QRT-PCR detected mRNA expression; (**C**) The proliferation of cell lines tested by CCK-8 assay; (**D**) The expression of α-SMA in the cell lines after lentiviral infection and puromycin sceening tested by immunofluorescence (×200). The red fluorescence represented α-SMA signals, and the blue fluorescence represented nucleus. (**E**) The content of hydroxyproline (HYP) in the cell lines after lentiviral infection and puromycin screening.

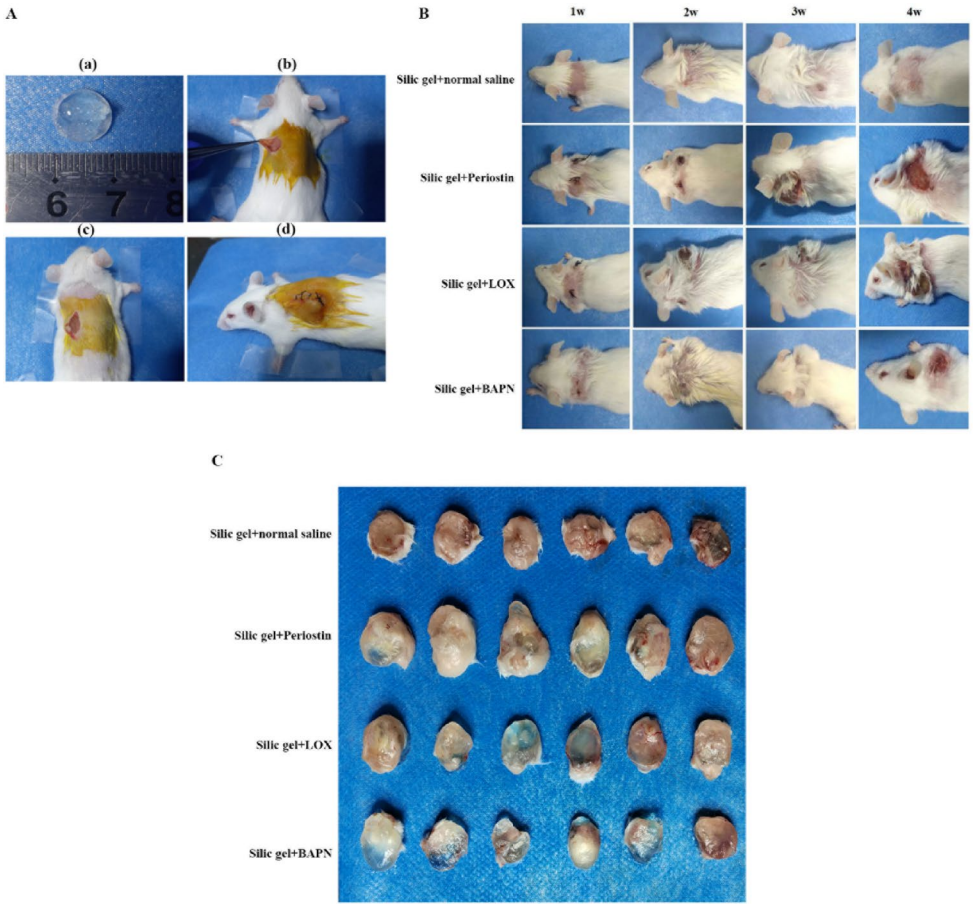

Fig. 5. The diagram of mouse model of prosthesis implantation with periostin, LOX and BAPN treatment. (**A**) Modeling process diagram. (a) Hemispherical silicone prosthesis; (b) Cut skin into bags; (c) Implant spherical silicone prosthesis; (d) Suture and disinfect the skin. (**B**) Process record chart. The silica gel + LOX group had the slowest wound healing and more severe suppurative condition. (**C**) General drawing of silicone implants. The silica gel + periostin group had a larger prosthesis block and the surrounding tissues were yellow.

extent of capsular contracture. In vitro experiments demonstrated that periostin promotes the proliferation of human breast fibroblasts, regulates fibrosis-related cytokine expression, induces fibroblasts to express α-SMA and differentiate into myofibroblasts, and stimulates collagen production. Furthermore, our findings were validated in a mouse model of prosthesis implantation, where we observed reduced capsule thickness with LOX inhibitors. To our knowledge, this study represents the first comprehensive investigation into the role of periostin in capsule formation, both in vitro and in vivo.

Early studies have explored the role of TGF-β in breast prosthesis capsule formation, indicating its pivotal involvement in fibrosis initiation[21–25]. Subsequent investigations demonstrated that periostin, a downstream protein in the TGF-β signaling pathway, plays a crucial role in various fibrotic diseases. In a study of the mouse model of muscle atrophy, Lorts et al. found that in the absence of periostin, the TGF-β pathway was changed to support regeneration but not increase fibrosis. Therefore, targeting periostin downstream of TGF-β may offer therapeutic advantages over targeting the entire TGF-β pathway[26]. Moreover, in a study of primary pulmonary fibrosis, CP4715, an inhibitor of periostin receptor $\alpha_V\beta_3$ integrin, successfully blocked the interaction between TGF-β and periostin, becoming a potential therapeutic target for pulmonary fibrosis[27]. Some preliminary studies have shown that periostin and LOX are expressed in capsular tissues[16,20]inspiring speculation regarding their role in breast prosthesis capsule formation and contracture. In clinical capsular specimens, immunohistochemistry demonstrated that the expression of periostin and other fibrosis related proteins were correlated with the degree of capsular contracture. This confirms our hypothesis that periostin may play an important role in capsule formation and contracture after breast prosthesis implantation. We further confirmed our hypothesis at the cellular level and in animal models.

In the study of cell proliferation using CCK8 experiment, the data of this study showed that periostin can promote the proliferation activity of breast derived fibroblasts, and the difference was more obvious after 24 h. Previous studies have linked fibroblast porliferation to TGF-β signaling. Thevenot et al. confirmed the relationship between mast cells and prosthesis formation in the subcutaneous prosthesis model[28]. Brazin et al. further demonstrated that the number of fibroblasts in the capsule was related to the degree of capsule contracture, and this correlation was derived from the fact that TGF-β secreted by mast cells stimulated fibroblast proliferation

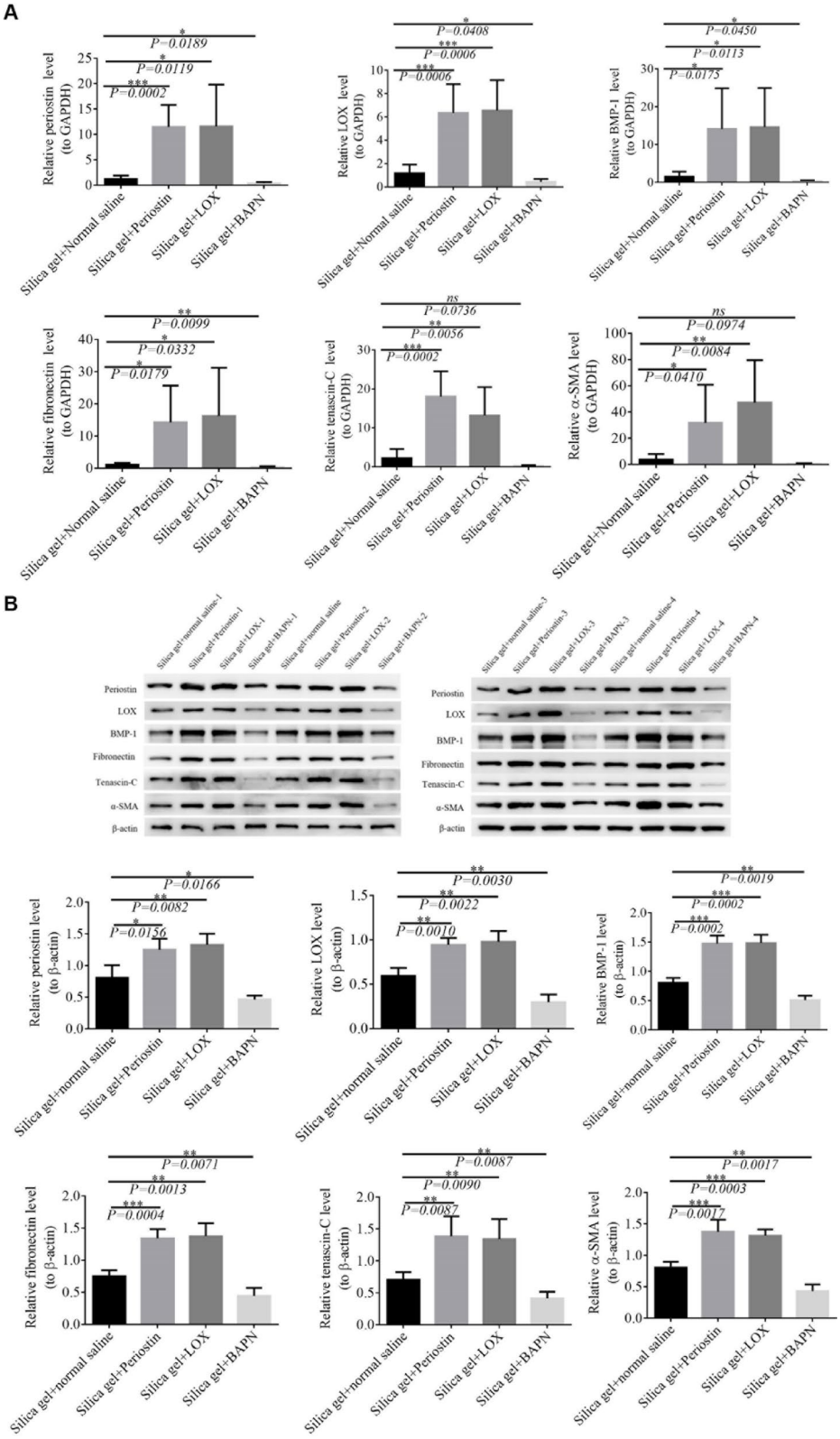

Fig. 6. The expression of periostin and other fibrosis related genes in the prosthesis capsules of mouse model with periostin, LOX and BAPN treatment ($N = 24$). (**A**) Statistical histogram of qPCR detection of periostin, LOX, BMP-1, fibronectin, tenascin-C and α-SMA in 4 groups; (**B**) Western blotting detection of 6 proteins in 4 groups. *$P<0.05$, ** $P<0.01$, *** $P<0.005$.

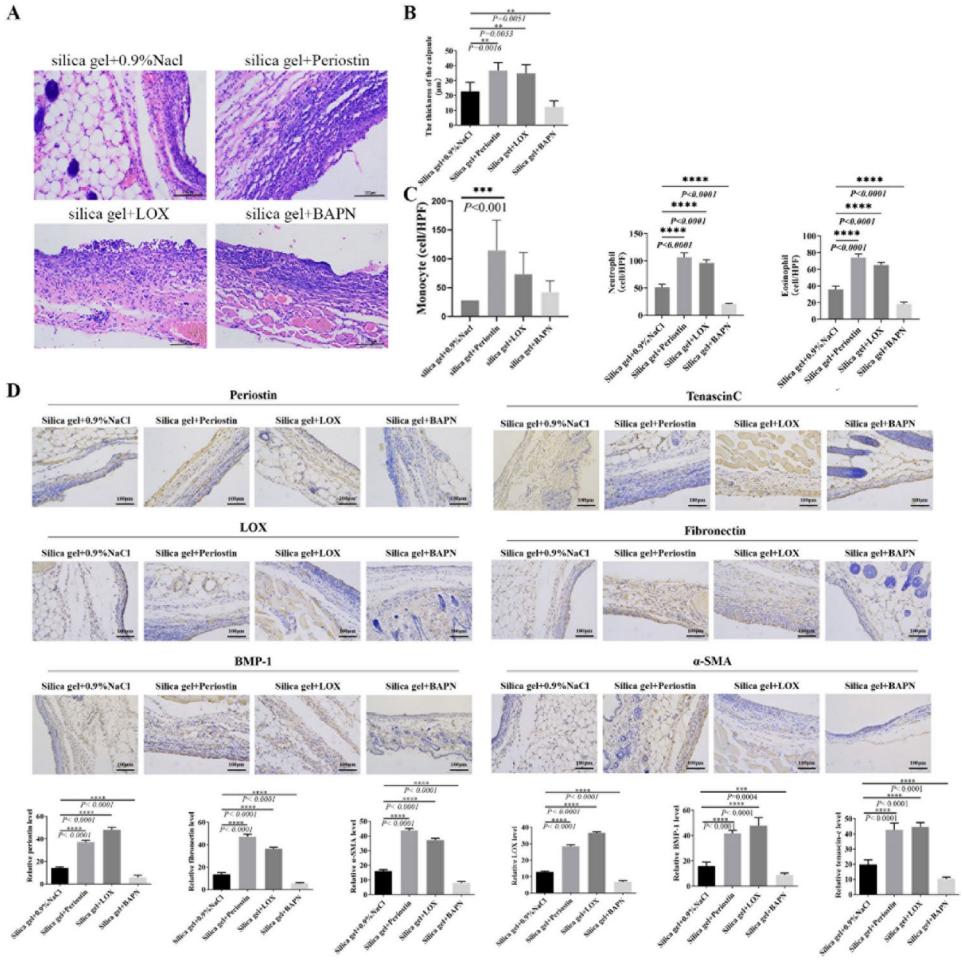

Fig. 7. The thickness, the number of imflammatory cells and the expression of immunohistochemical markers of the mouse model capsules treated with periostin, LOX and BAPN ($N=24$). (**A**) The microscopic images of the implants capsules in the 4 groups. (**B**) The thickness of the implants capsules in the 4 groups. (**C**) The number of neutrophils, eosinophils, and monocytes in the 4 groups. (**D**) The immunohistochemical expression of periostin, LOX, BMP-1, fibronectin, tenascin-C and α-SMA of the capsules in the 4 groups. *$P<0.05$, ** $P<0.01$, *** $P<0.005$.

and collagen formation[29]. Notably, our study suggested that periostin, downstream of TGF-β, contributes to fibroblast proliferation, potentially exacerbating capsule formation and contracture.

Existing studies have preliminarily understood the mechanism of periostin in the process of bone, tooth, heart and skin fibrosis. In response to inflammation and mechanical pressure, the expression of periostin and other extracellular matrix molecules are triggered by cytokines secreted by immune cells, promoting extracellular matrix (ECM) remodeling[30]. Periostin interacts with integrins on myofibroblasts, facilitating cell migration and ECM assembly[31]. Periostin induces the expression of intercellular and extracellular type I collagen and fibronectin[32], it also constitutes a scaffold structure with tenascin-C and fibronectin to interact with type I collagen[31]. Moreover, periostin supports BMP-1-mediated LOX activation, enhancing collagen cross-linking[15]. Combined with the above studies, our study detected the expression of some key genes related to fibrosis in human breast derived fibroblasts overexpressing and interfering with periostin. Our results, consistent with those of previous studies, showed that BMP-1, LOX, fibronectin and tenascin-C are closely related to the expression of periostin, which increase with the expression of periostin and decrease with the interference of periostin. Among the four genes, tenascin-C was most significantly affected by periostin overexpression, and BMP-1 was most significantly affected by periostin interference.

Collagen fibers undergo stabilization through covalent cross-linking, a process initiated by the oxidation of lysine residues by LOX enzymes. This enzymatic activity removes residual lysine or hydroxylysine from collagen fiber tails, facilitating the formation of sponge-like cross-links between adjacent collagen molecules. These bivalent cross-links mature into more stable trivalent forms over time[33,34]. LOX activity not only influences the shape of collagen fibers but also contributes to the complex layered structure observed in tissues such as the cornea[35]. Consequently, LOX-mediated covalent cross-linking is a crucial step in collagen formation, ultimately determining the mechanical properties of the extracellular matrix. Studies in periostin-deficient mice and post-myocardial infarction heart tissues have highlighted the common occurrence of collagen cross-linking

abnormalities[36]underscoring the essential role of periostin in establishing and maintaining connective tissue mechanical properties. Kumar et al. found that periostin promotes enhanced matrix stiffness in chronic liver disease by activating LOX and LOXL, independently of TGF-β receptors[32]. In terms of specific mechanism research, Maruhashi et al. confirmed that periostin supports the hydrolysis activation of LOX mediated by BMP-1 in the extracellular matrix, thereby strengthening the cross-linking of collagen[15]. Radhakrishnan et al. Demonstrated that periostin regulates the activation of LOX in cardiac fibroblasts through ERK1/2 MAPK dependent serum reactive factor, thereby increasing collagen cross-linking after heart failure[37]. Our study further corroborated this relationship, showing significant changes in LOX expression following periostin modulation. Additionally, periostin-overexpressing cells exhibited elevated hydroxyproline levels, a marker of collagen production[38] suggesting a role for periostin in promoting collagen synthesis. Of course, the production and deposition/cross-linking of collagen are two different concepts. Our experiment only confirmed that periostin promotes collagen production, and further research is needed to determine whether it has an impact on collagen deposition and/or cross-linking.

Myofibroblasts, contractile fibroblasts crucial for wound healing, are commonly observed within breast prosthesis capsules[39]. These cells arise from fibroblast differentiation under appropriate stimulation and subsequently generate contractile forces to facilitate wound closure[40]. α-SMA serves as a marker of myofibroblast differentiation[41] and is associated with the degree of capsule contracture[7]. Bui et al. believed that the continuous activation of fibroblasts and myofibroblasts may cause the contracture of prosthesis capsule[7] while antagonising the estrogen of myofibroblasts can alleviate the severity of contracture[42]. Previous studies have found that periostin can regulate the expression of the downstream gene α-SMA[11,43]. In periostin silenced mice, the number of α-SMA positive myofibroblasts in lung tissue decreased, thus avoiding hyperoxia mediated pulmonary interstitial fibrosis[44]. Our study, consistent with previous findings, revealed an increase in α-SMA expression with worsening capsule contracture, both in clinical specimens and periostin-overexpressing fibroblasts. Hence, periostin's regulation of downstream α-SMA expression likely contributes to myofibroblast differentiation during breast prosthesis capsule formation.

In animal models, periostin and LOX were found to increase capsule thickness, whereas LOX inhibition significantly reduced thickness. These findings were consistent with in vitro results demonstrating changes in fibrosis-related gene and protein expression. Some researchers have demonstrated that knockdown of LOX expression or inhibition of LOX activity alleviates the lung fibrosis[45]. Our study is the first to utilize a LOX inhibitor to mitigate fibrosis in a prosthesis implantation model, indicating the potential possibility of clinical application to reduce capsule contracture. However, unexpected outcomes, including severe inflammation and delayed wound healing in periostin and LOX treatment groups, underscore the complexities of their roles in tissue repair and inflammation. The role of periostin in inflammation and tissue repair has been studied for many years[46–48]. Some researchers found that regeneration and repair is delayed in the absence of periostin[49,50]. LOX is also considered to be a promoter of tissue repair after injury[51]. A few investigators have reported some approaches to accelerating healing of injured tissues through up-regulating the LOX in the acute phase after injury[52]. Our findings challenge this notion, highlighting the need for further research to elucidate the precise roles of periostin and LOX in inflammation and tissue repair processes.

Collectively, our findings and existing evidence indicate that periostin plays a pivotal role in breast implant-associated capsular fibrosis and contracture through interconnected mechanisms. Following surgical injury, inflammation, and mechanical stress from the implant, periostin expression is robustly induced, primarily by immune cell-derived cytokines, and secreted into ECM. Periostin subsequently mediates the upregulation of key profibrotic factors, including BMP-1, LOX, Tenascin C, and fibronectin, while directly stimulating collagen production. Crucially, periostin-induced BMP-1 facilitates the activation of LOX, enhancing collagen cross-linking and ECM stabilization. Furthermore, periostin promotes the assembly of type I collagen, Tenascin C, and fibronectin into a dense, organized scaffold essential for capsule formation. Concurrently, periostin drives fibroblast proliferation and their differentiation into contractile myofibroblasts, the primary effectors of capsule contraction. This coordinated action on both ECM organization and cellular phenotype establishes periostin as a central regulator in the pathogenesis of capsular fibrosis.

This study still has limitations. Firstly, it only preliminarily observed the role of periostin in the formation of breast prosthesis capsule, and did not reveal its specific mechanism of action; Secondly, there was no rescue experiment in animal experiments, which resulted in a lack of direct evidence for the relationship between periostin and LOX; Thirdly, this study only conducted a single line analysis of the role of periostin, lacking research on the network interaction relationships of multiple molecular pathways. These will serve as the next direction for this study.

Conclusions

Our study sheds light on the critical role of periostin in breast prosthesis capsule formation and contracture mechanisms. By regulating other fibrosis-related genes, promoting fibroblasts proliferation, influencing collagen production and myofibroblasts differentiation, periostin emerges as a potential therapeutic target for mitigating capsule contracture in breast augmentation patients, warranting further investigation into its specific mechanisms and clinical applications.

Data availability

all data generated or analysed during this study are included in this published article and its supplementary information files.

Received: 7 June 2024; Accepted: 10 July 2025

Published online: 15 July 2025

References

1. Headon, H. K. A. & Mokbel, K. Capsular contracture after breast augmentation: an update for clinical practice. *Arch. Plast. Surg.* **42**, 532–543 (2015).
2. Ali, A., Picado, O., Mathew, P. J., Ovadia, S. & Thaller, S. R. Risk factors for capsular contracture in alloplastic reconstructive and augmentation mammaplasty: analysis of the National surgical quality improvement program (NSQIP) database. *Aesthetic Plast. Surg.* **47**, 1678–1682 (2023).
3. Steiert, A. E. B. M. & Sorg, H. Capsular contracture by silicone breast implants: possible causes, biocompatibility, and prophylactic strategies. *Med. Devices (Auckl).* **6**, 211–218 (2013).
4. Coombs, D. M., Grover, R., Prassinos, A. & Gurunluoglu, R. Breast augmentation surgery: clinical considerations. *Cleve. Clin. J. Med.* **86**, 111–122 (2019).
5. Prantl, L. S. S. et al. Clinical and morphological conditions in capsular contracture formed around silicone breast implants. *Plast. Reconstr. Surg.* **120**, 275–284 (2007).
6. Rocco, N. R. C. et al. Different types of implants for reconstructive breast surgery. *Cochrane Database Syst. Rev.* **16**, CD010895 (2016).
7. Bui, J. M. P. T., Ren, C. D., Nofrey, B., Teitelbaum, S. & Van Epps, D. E. Histological characterization of human breast implant capsules. *Aesthetic Plast. Surg.* **39**, 306–315 (2015).
8. Kim, C. H. K., Oh, D. H. & Song, S. H. Human embryonic stem cell-derived endothelial precursor cell conditioned medium reduces the thickness of the capsule around silicone implants in rats. *Ann. Plast. Surg.* **75**, 348–352 (2015).
9. Achilles, R. B. et al. Cytotoxicity, inflammatory activity, and angiogenesis are induced by different silicone implants. *In vivo*. 36, 1252–1258 (2022).
10. Bérniz, C. et al. Breast implant capsule: A murine model comparing capsular contracture susceptibility among six breast implants available in the market. *Aesthetic Plast. Surg.* **47**, 2093–2105 (2023).
11. Conway, S. J. I. K. et al. The role of Periostin in tissue remodeling across health and disease. *Cell. Mol. Life Sci.* **71**, 1279–1288 (2014).
12. Liu, A. Y. Z. H. & Ouyang, G. Periostin, a multifunctional matricellular protein in inflammatory and tumor microenvironments. *Matrix Biol.* **37**, 150–156 (2014).
13. Kormann, R. et al. Periostin promotes cell proliferation and macrophage polarization to drive repair after AKI. *J. Am. Soc. Nephrology: JASN*. **31**, 85–100 (2020).
14. Lee, Y. J. K. I. et al. Periostin-binding DNA aptamer inhibits breast cancer growth and metastasis. *Mol. Ther.* **21**, 1004–1013 (2013).
15. Maruhashi, T., Kii, I., Saito, M. & Kudo, A. Interaction between periostin and BMP-1 promotes proteolytic activation of Lysyl oxidase. *J. Biol. Chem.* **285**, 13294–13303 (2010).
16. Poh, P. S. P. et al. Non-linear optical microscopy and histological analysis of collagen, elastin and lysyl oxidase expression in breast capsular contracture. *Eur. J. Med. Res.* **23**, 30 (2018).
17. de Bakker, E. et al. The Baker classification for capsular contracture in breast implant surgery is unreliable as a diagnostic tool. *Plast. Reconstr. Surg.* **146**, 956–962 (2020).
18. Larsen, A. et al. Development and validation of a diagnostic histopathological scoring system for capsular contracture based on 720 breast implant capsules. *Aesthet. Surg. J.* **44**, NP391–NP401 (2024).
19. Larsen, A. et al. A histological assessment tool for breast implant capsules validated in 480 patients with and without capsular contracture. *Aesthetic Plast. Surg.* **49**, 497–508 (2025).
20. Bae, H. S., Son, H. Y., Lee, J. P., Chang, H. & Park, J. U. The role of periostin in capsule formation on silicone implants. *BioMed Res. Int.* **2018**, 3167037 (2018).
21. Kuhn, A. et al. Periprosthetic breast capsules contain the fibrogenic cytokines TGF-beta1 and TGF-beta2, suggesting possible new treatment approaches. *Ann. Plast. Surg.* **44**, 387–391 (2000).
22. Ruiz-de-Erenchun, R., Dotor de las Herrerias, J. & Hontanilla, B. Use of the transforming growth factor-beta1 inhibitor peptide in periprosthetic capsular fibrosis: experimental model with tetraglycerol dipalmitate. *Plast. Reconstr. Surg.* **116**, 1370–1378 (2005).
23. Schlesinger, S. L., Ellenbogen, R., Desvigne, M. N., Svehlak, S. & Heck, R. Zafirlukast (Accolate): A new treatment for capsular contracture. *Aesthet. Surg. J.* **22**, 329–336 (2002).
24. Katzel, E. B. K. P. et al. The impact of Smad3 loss of function on TGF-β signaling and radiation-induced capsular contracture. *Plast. Reconstr. Surg.* **127**, 2263–2269 (2011).
25. Zeplin, P. H. L. A. A. & Schmidt, K. Surface modification of silicone breast implants by binding the antifibrotic drug halofuginone reduces capsular fibrosis. *Plast. Reconstr. Surg.* **126**, 266–274 (2010).
26. Lorts, A. S. J., Baudino, T. A., McNally, E. M. & Molkentin, J. D. Deletion of periostin reduces muscular dystrophy and fibrosis in mice by modulating the transforming growth factor-β pathway. *Proc. Natl. Acad. Sci. U S A*. **109**, 10978–10983 (2012).
27. Nanri, Y. et al. Cross-talk between transforming growth factor-β and periostin can be targeted for pulmonary fibrosis. *Am. J. Respir. Cell Mol. Biol.* **62**, 204–216 (2020).
28. Thevenot, P. T., Baker, D. W., Weng, H., Sun, M. W. & Tang, L. The pivotal role of fibrocytes and mast cells in mediating fibrotic reactions to biomaterials. *Biomaterials* **32**, 8394–8403 (2011).
29. Brazin, J. M. S. et al. Mast cells in the periprosthetic breast capsule. *Aesthetic Plast. Surg.* **38**, 592–601 (2014).
30. Chiquet, M. G. L., Lutz, R. & Maier, S. From mechanotransduction to extracellular matrix gene expression in fibroblasts. *Biochim. Biophys. Acta*. **1793**, 911–920 (2009).
31. K, A. Periostin in fibrillogenesis for tissue regeneration: Periostin actions inside and outside the cell. *Cell. Mol. Life Sci.* **68**, 3201–3207 (2011).
32. Kumar, P. et al. Periostin promotes liver fibrogenesis by activating lysyl oxidase in hepatic stellate cells. *J. Biol. Chem.* **293**, 12781–12792 (2018).
33. Bella, J. & Hulmes, D. J. Fibrillar collagens. *Sub-cellular Biochem.* **82**, 457–490 (2017).
34. Vallet, S. D. & Ricard-Blum, S. Lysyl oxidases: from enzyme activity to extracellular matrix cross-links. *Essays Biochem.* **63**, 349–364 (2019).
35. Herchenhan, A. U. F. et al. Lysyl oxidase activity is required for ordered collagen fibrillogenesis by tendon cells. *J. Biol. Chem.* **290**, 16440–16450 (2015).
36. Shimazaki, M. N. K. et al. Periostin is essential for cardiac healing after acute myocardial infarction. *J. Exp. Med.* **205**, 295–303 (2008).
37. Radhakrishnan, S. et al. Periostin regulates lysyl oxidase through ERK1/2 MAPK-dependent serum response factor in activated cardiac fibroblasts. *Cell Biochem. Funct.* **42**, e4066 (2024).
38. Wang, Z. & Chesler, N. C. Role of collagen content and cross-linking in large pulmonary arterial stiffening after chronic hypoxia. *Biomech. Model. Mechanobiol.* **11**, 279–289 (2012).
39. Hwang, K., Sim, H. B., Huan, F. & Kim, D. J. Myofibroblasts and capsular tissue tension in breast capsular contracture. *Aesthetic Plast. Surg.* **34**, 716–721 (2010).
40. Baker, J. L. Jr., Chandler, M. L. & LeVier, R. R. Occurrence and activity of myofibroblasts in human capsular tissue surrounding mammary implants. *Plast. Reconstr. Surg.* **68**, 905–912 (1981).

41. Powell, D. W. Myofibroblasts: paracrine cells important in health and disease. *Trans. Am. Clin. Climatol. Assoc.* **111**, 271–292 (2000). discussion 92 – 3.
42. Persichetti, P. et al. Oestrogen receptor-alpha and -beta expression in breast implant capsules: experimental findings and clinical correlates. *J. Plast. Reconstr. Aesthet. Surg.* **67**, 308–315 (2014).
43. Ashley, S. L., Wilke, C. A., Kim, K. K. & Moore, B. B. Periostin regulates fibrocyte function to promote myofibroblast differentiation and lung fibrosis. *Mucosal Immunol.* **10**, 341–351 (2017).
44. Bozyk, P. D. B. J. et al. Neonatal periostin knockout mice are protected from hyperoxia-induced alveolar simplication. *PLoS One.* **7**, e31336 (2012).
45. Cheng, T. L. Q. et al. Lysyl oxidase promotes bleomycin-induced lung fibrosis through modulating inflammation. *J. Mol. Cell. Biol.* **6**, 506–515 (2014).
46. Sonnenberg-Riethmacher, E., Miehe, M. & Riethmacher, D. Periostin in allergy and inflammation. *Front. Immunol.* **12**, 722170 (2021).
47. Walker, J. T., McLeod, K., Kim, S., Conway, S. J. & Hamilton, D. W. Periostin as a multifunctional modulator of the wound healing response. *Cell Tissue Res.* **365**, 453–465 (2016).
48. Yang, L., Guo, T., Chen, Y. & Bian, K. The multiple roles of periostin in non-neoplastic disease. *Cells* **12**. (2022).
49. Nishiyama, T. et al. Delayed re-epithelialization in periostin-deficient mice during cutaneous wound healing. *PLoS One.* **6**, e18410 (2011).
50. Shih, C. H., Lacagnina, M., Leuer-Bisciotti, K. & Pröschel, C. Astroglial-derived periostin promotes axonal regeneration after spinal cord injury. *J. Neuroscience: Official J. Soc. Neurosci.* **34**, 2438–2443 (2014).
51. Cai, L. X. X., Kong, X. & Xie, J. The role of the lysyl oxidases in tissue repair and remodeling: A concise review. *Tissue Eng. Regen Med.* **14**, 15–30 (2017).
52. Pathi, S. D. et al. Recovery of the injured external anal sphincter after injection of local or intravenous mesenchymal stem cells. *Obstet. Gynecol.* **119**, 134–144 (2012).

Author contributions

Ying Yang conceived and supervised the study. Shumo Li designed experiments. Li Bian performed clinico-pathological eveluation. Jun Hu and Li Bian performed cell culture and molecular analysis. Ying Yang wrote the manuscript. Ying Yang and Li Bian interpreted the data. Shumo Li , Xiaoming Dai, Yun Ma carried out patient data collection. Zhiyuan Wang performed bioinformatics and statistical analyses. All authors read and approved the final manuscript.

Funding

This research was funded by Joint Projects of Applied Basic Research of Kunming Medical University and Yunnan Province Department of Science and Technology (202101AY070001-109), and First-Class Discipline Team of Kunming Medical University (2024XKTDTS11).

Declarations

Competing interests

The authors declare no competing interests.

Additional information

Supplementary Information The online version contains supplementary material available at https://doi.org/10.1038/s41598-025-11409-9.

Correspondence and requests for materials should be addressed to Y.Y.